Dalton Transactions

ROYAL SOCIETY OF CHEMISTRY

PAPER

View Article Online
View Journal | View Issue



Cite this: *Dalton Trans.*, 2026, **55**, 8128

# Resistance to nitrogen-induced catalytic deactivation in VGO cracking: synergistic effect of hierarchical structuring and zeolite Y content in FCC catalysts

Jayson Fals, *[a,b] María L. Ospina-Castro,[c,d] Clara Barragán-Avilez,[e] Roger Valle-Molinares, [f] Dary Mendoza,[b] Jhonnys D. Guerrero,[g,h] Sonia Bocanegra[h] and Fabián Espitia-Almeida *[e]

In this study, four FCC catalysts were synthesized by varying both the zeolite Y content (30 wt% and 40 wt%) and the degree of structural modification through alkaline desilication, aiming to evaluate their resistance to nitrogen-induced catalytic deactivation during the cracking of Colombian vacuum gas oil (VGO). The generation of hierarchical zeolites with intracrystalline mesoporosity enabled their subsequent incorporation into catalyst formulations with different active phase loadings. To simulate severe deactivation conditions, quinoline and indole were added to the VGO as model ni-trogen-containing compounds with distinct basicity. Catalytic performance was assessed in a fixed-bed MAT reactor, analyzing conversion, product distribution and quality, coke deposition, as well as the evolution of textural and acidic properties. The results revealed a synergistic effect between zeolite hierarchization and its loading in the catalyst, leading to enhanced nitrogen tolerance, improved structural stability, and increased resistance to coke-induced deactivation. Specifically, systems containing hierarchical zeolite with higher active phase content exhibited better preservation of Brønsted acidity and reduced coke formation, underscoring the importance of multiscale pore design in mitigating inhibitory effects from nitrogen species. This study provides experimental evidence of the critical role of intracrystalline mesoporosity and zeolite content in determining FCC catalyst performance under severe chemical deactivation scenariosstract text goes here.

Received 16th December 2025,
Accepted 31st January 2026

DOI: 10.1039/d5dt02992a

rsc.li/dalton



## 1. Introduction

Catalytic cracking of vacuum gas oil (VGO) is one of the main technologies employed in the refining industry for the conversion of heavy petroleum fractions into lighter, high-er-value products such as gasoline, liquefied gases, and olefins.[1–3] This process, typically conducted in Fluid Catalytic Cracking (FCC) units, relies on composite catalysts containing Y zeolite as the active phase, dispersed within a matrix composed of silica, alumina, and clays.[4–7] Y zeolite, due to its high Brønsted acidity and microporous framework, enables selective cracking reactions of the large molecules present in VGO.[8,9] However, the presence of nitrogen-containing compounds in the feedstock poses a significant challenge, as these basic species can neutralize or block the acidic sites of the catalyst, thereby adversely affecting its activity, selectivity, and stability. This type of chemical deactivation is particularly problematic when processing heavy and extra heavy crude oils, such as many of those found in Latin America, which often contain elevated concentrations of organic nitrogen in the form of heterocyclic

[a]*Grupo de Investigación en Oxi/Hidrotratamiento Catalítico y Nuevos Materiales, Programa de Química-Ciencias Básicas, Universidad del Atlántico, Puerto Colombia 081001, Colombia. E-mail: jaysonfals@mail.uniatlantico.edu.co*
[b]*Grupo de Productos Naturales y Bioquímica de Macromoléculas, Universidad del Atlántico, Facultad de Ciencias, Puerto Colombia 081001, Colombia*
[c]*Grupo de Investigación en Química Supramolecular Aplicada, Programa de Química, Facultad de Ciencias Básicas, Universidad del Atlántico, Puerto Colombia 081001, Colombia*
[d]*Programa de Química, Facultad de Ciencias Básicas, Universidad del Atlántico, Puerto Colombia 081001, Colombia*
[e]*Centro de Investigaciones en Ciencias de la Vida, Facultad de Ciencias Básicas y Biomedicas, Universidad Simón Bolívar, Barranquilla 080002, Colombia. E-mail: fabian.espitia@unisimon.edu.co*
[f]*Facultad de Ciencias Básicas, Programa de Biología, Universidad del Atlántico, Puerto Colombia 081001, Colombia*
[g]*Grupo de Investigación en Biotecnología de Microalgas, Fisicoquímica Aplicada y Estudios Ambientales, Programa de Química, Universidad del Atlántico, Puerto Colombia 080003, Colombia*
[h]*Instituto de Investigaciones en Catálisis y Petroquímica (INCAPE)/Consejo Nacional de Investigaciones Científicas y Técnicas (CONICET), Universidad Nacional del Litoral, Santa Fe CP 3000, Argentina*

aromatic compounds (*e.g.*, quinolines, pyridines, and indoles). These species not only compete for the active sites but also promote coke formation, thereby reducing catalyst lifetime and leading to substantial operational losses in the FCC unit.[10–12]

Several studies in the literature have reported the detrimental impact of nitrogen containing compounds on the activity of FCC catalysts, which is primarily attributed to the basic affinity of these molecules for Brønsted acid sites, responsible for initiating cracking reactions. Their preferential adsorption leads to a significant loss of available acidity, reduced VGO conversion, and alterations in product distribution.[13–15] Additionally, these compounds may promote coke formation, thereby accelerating both thermal and chemical catalyst deactivation.[16] Although various strategies have been proposed to mitigate this effect such as modifying acidity or incorporating neutralizing additives most of them show limitations under real operating conditions, particularly when processing feedstocks with high nitrogen content.[17] In this context, it becomes crucial to develop catalysts that not only retain their activity in the presence of basic species but also maintain structural stability and regenerability over multiple reaction/regeneration cycles.[18] The need for robust solutions is further emphasized by the growing interest in pro-cessing heavy and unconventional crudes, which are abundant in regions such as South America and impose more demanding conditions on conventional catalytic systems.

In response to this challenge, recent research in the field of heterogeneous catalysis has focused on structural modification of Y zeolite as an effective strategy to enhance catalytic activity and improve resistance to deactivation. Zeolite hierarchization *via* alkaline treatment enables the development of a bimodal pore network that combines inherent microporosity with accessible mesopores, thereby facilitating the diffusion of bulky VGO molecules and reducing blockage of active sites by coke. The generated mesoporosity not only improves accessibility to acid sites but also contributes to more efficient catalyst regeneration. Additionally, the alkaline treatment can preserve or even enhance Brønsted acidity in structurally modified regions, which is essential to maintain high catalytic activity under severe operating conditions. In addition, the Y zeolite content in the catalytic formulation is another critical factor, as a higher proportion of active phase may compensate for the loss of acid sites caused by basic compounds, improving conversion and selectivity toward light products.[19–21] However, the synergistic combination of these two strategies hierarchization and zeolite content, has not been thoroughly explored, particularly under conditions simulating the processing of VGO with high levels of organic nitrogen. In this context, it becomes relevant to investigate how the interaction between hierarchical structure and Y zeolite concentration in the catalyst may enhance chemical resistance to deactivation, thereby contributing to the design of more robust, efficient, and industry-adapted catalytic formulations.

The formulation of new catalysts and the impact of feedstock properties must be evaluated at the laboratory scale. This evaluation phase is essential to understand the individual and combined effects of catalytic and feedstock variables, allowing the simulation of representative industrial operating conditions under rigorous experimental control. Among the most widely used evaluation reactors is the fixed bed Micro Activity Test (MAT) unit, which is extensively employed in FCC studies due to its ability to replicate the thermal and catalytic conditions of the process. This facilitates direct comparison of catalytic formulations in terms of conversion, product distribution, and resistance to deactivation. The MAT reactor is a key tool for generating reliable laboratory scale data that can serve as a foundation for subsequent validation at pilot and, eventually, industrial scales.[22,23] Implementing these sequential analysis stages minimizes operational risks and prevents the need for costly direct plant testing, thereby ensuring a more efficient and well-supported transition toward catalytic solutions applicable to real-world refining environments.

Catalyst deactivation caused by nitrogen containing compounds in vacuum gas oil (VGO) remains a critical challenge in catalytic cracking processes. The development of composite catalysts formulated with varying proportions of hierarchical Y zeolite has emerged as a promising strategy to enhance catalytic performance when processing heavy feedstocks. The incorporation of hierarchical zeolites not only aims to mitigate the effects of chemical deactivation, but also to optimize the accessibility to acid sites and improve catalyst regenerability. This study aims to evaluate the catalytic behaviour of FCC formulations incorporating different concentrations of hierarchical Y zeolite in response to a typical Colombian VGO feedstock contaminated with representative nitrogen compounds, such as quinoline and indole. The objective is to determine the effect of these variables on conversion, product distribution, and resistance to deactivation using a laboratory-scale MAT reactor. The results will provide insights for designing more robust and efficient catalysts tailored for the processing of heavy fractions with challenging compositions, aligning with the current demands of the refining industry in regions rich in unconventional crude oils.

## 2. Results and discussion

### 2.1. Feedstocks

In order to determine the composition of the feedstock (VGOs doped with varying concentrations of quinoline and indole) and to detect potential contaminant species that may impair catalytic activity, a comprehensive characterization of the feed is required using advanced analytical techniques. Table 1 summarizes the properties of the raw materials used in this research. The API gravity value obtained for the VGO feedstock (API = 18.5) classifies it as a heavy fraction, consistent with those reported for feeds derived from heavy crude oils.[24] This low relative density is directly related to its high content of aromatic compounds (>48 wt%), which increases bulk density and consequently lowers the API gravity. The elevated aromaticity, particularly the presence of polycyclic aromatic hydro-

**Table 1** Physicochemical and elemental properties of the VGO feedstock

| Feedstock | VGO | VGO01 | VGO02 | VGO03 |
|---|---|---|---|---|
| API | 18.5 | — | — | — |
| Aniline point (°C) | 76.9 | — | — | — |
| CCR (wt%) | 0.46 | — | — | — |
| Refractive index | 1.4930 | — | — | — |
| Distillation curve (°C) | | — | — | — |
| Initial | 270 | — | — | — |
| 10 vol% | 376 | — | — | — |
| 30 vol% | 415 | — | — | — |
| 50 vol% | 446 | — | — | — |
| 70 vol% | 481 | — | — | — |
| 95 vol% | 529 | — | — | — |
| Final | 575 | — | — | — |
| SARA fractions (wt%) | | — | — | — |
| Saturated | 49.1 | — | — | — |
| Aromatic | 48.5 | — | — | — |
| Resin | 1.90 | — | — | — |
| Asphaltene | 0.50 | — | — | — |
| Nickel (ppm) | 0.55 | — | — | — |
| Vanadium (ppm) | 0.86 | — | — | — |
| Sodium (ppm) | 0.91 | — | — | — |
| Iron (ppm) | 0.30 | — | — | — |
| Quinoline (wt%) | — | 0.40 | 0.00 | 0.40 |
| Indol (wt%) | — | 0.00 | 0.40 | 0.40 |
| Nitrogen total (wt%) | 0.10 | 0.50 | 0.50 | 0.90 |

carbons, not only affects the physicochemical properties of the feed but also plays a critical role in catalytic cracking reactivity, promoting coke formation and negatively impacting catalyst stability.

The physicochemical and elemental properties of the original VGO confirm its classification as a heavy fraction, with significant implications for its behaviour in catalytic cracking processes. The aniline point (76.9 °C) and refractive index (1.4930) are consistent with a feedstock rich in aromatic compounds, as supported by the compositional analyzis (48.5 wt% aromatics and 49.1 wt% saturates). Although the Conradson carbon residue (CCR = 0.46 wt%) indicates a low tendency toward coke formation under thermal conditions, the high aromaticity may promote coke generation under catalytic conditions.

The resin (1.90 wt%) and asphaltene (0.50 wt%) contents are relatively low, suggesting moderate colloidal stability and a low risk of pore blockage in the catalyst by heavy polar species.[25,26] The total nitrogen content (0.18 wt%) falls within the typical range for VGOs, yet it may still interfere with the catalysts acid sites, particularly Brønsted type sites, leading to temporary or permanent deactivation through competitive adsorption or poisoning.[27] Regarding trace metals, the concentrations of nickel (0.55 ppm), vanadium (0.86 ppm), sodium (0.91 ppm), and iron (0.30 ppm) are low, indicating a limited risk of metal-induced dehydrogenation, coke formation, or structural damage to the zeolite framework.[28]

The distillation curve obtained further confirms the heavy nature of the feedstock, with an initial boiling point of 270 °C and 95 vol% distilled below 529 °C, reaching a final boiling point of 575 °C. This broad boiling range, particularly the presence of high-boiling fractions, indicates a high molecular complexity that demands severe operating conditions or strong acidity for effective conversion.[29] Moreover, this complexity can influence both product selectivity and the rate of catalyst deactivation, especially in the presence of nitrogen containing compounds such as quinoline and indole.

Following the initial characterization of the VGO, and in order to investigate the deactivating effect of nitrogen containing compounds on catalysts formulated with hierarchical Y zeolite, a controlled doping strategy was implemented using quinoline and indole. Three doped feedstocks were prepared: VGO01, containing 0.40 wt% quinoline; VGO02, containing 0.40 wt% indole; and VGO03, containing 0.40 wt% of both compounds. As a result, the total nitrogen content increased to 0.50 wt% in VGO01 and VGO02, and up to 0.90 wt% in VGO03.

The presence of these two types of nitrogen-containing compounds is expected to negatively affect catalytic activity during cracking by competing for the catalysts acid sites, particularly Brønsted sites. Quinoline, due to its strong basic character, exhibits a higher affinity for these sites and may cause more pronounced chemical deactivation. In contrast, indole, which is a weaker base, may have a greater impact on physical deactivation by blocking access to the catalysts pores.[30]

### 2.2. Structural and textural characterization of the catalysts

The structural characterization of Y zeolites, before and after alkaline treatment, was conducted using X-ray diffraction (XRD) to evaluate potential changes in crystallinity and to indirectly confirm the formation of mesoporosity associated with hierarchical structuring. The emergence of mesopores typically manifests as a slight reduction in the intensity of the characteristic diffraction peaks, without significant disruption of the long-range structural order inherent to Y-type zeolites. As shown in Fig. 1, the XRD patterns of the untreated and treated zeolites both exhibit the distinctive reflections of the faujasite phase at $2\theta \approx 6.2°$, 10.2°, 15.7°, 23.6°, 27.1°, and 31.4°, indicating that the main crystalline frame-work is pre-

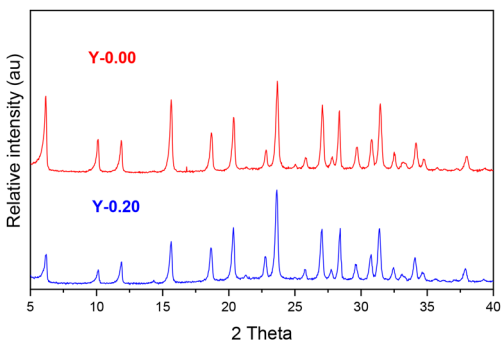


**Fig. 1** XRD patterns of Y zeolites before (Y-0.00) and after (Y-0.20) alkaline treatment.

served after modification. However, the treated sample displays a noticeable decrease in peak intensities, suggesting a minor loss of crystallinity attributable to partial desilication and dealumination induced by the alkaline treatment, a phenomenon commonly linked to mesopore formation and the development of hierarchical porosity.

This partial reduction in crystallinity is consistent with expectations for controlled desilication processes, where NaOH treatment generates intracrystalline mesoporosity within the zeolite, thereby promoting a hierarchical pore network without collapsing the faujasite lattice. The preservation of peak positions, combined with their attenuated intensity, supports the hypothesis that mesopores were introduced while retaining a substantial degree of structural order, an essential feature for ensuring sufficient accessibility to active sites without significantly compromising catalytic activity. It is important to note that XRD analyzis was conducted exclusively on the isolated zeolite powders. This decision was made because the relatively low zeolite content (30–40 wt%) in the composite catalysts, along with the amorphous nature of the binder and matrix components, tends to obscure the diffraction signals of the active phase, preventing accurate assessment of crystallinity in the final formulations.

Following the structural characterization, the textural properties of the zeolites and catalysts were evaluated by nitrogen physisorption at 77 K to quantify the porosity changes induced by the alkaline treatment. The parameters derived from the adsorption isotherms including specific surface area (BET), total pore volume ($V_{TP}$), micropore volume ($V_{micro}$), mesopore volume ($V_{meso}$), and average pore diameter (DP) are summarized in Table 2.

The parent zeolite (Y-0.00) exhibited typical microporous behaviour, with a moderately high BET surface area (718 $m^2$ $g^{-1}$) and a pore volume predominantly composed of micropores (0.381 $cm^3$ $g^{-1}$), accounting for approximately 70% of the total pore volume. Meso-porosity was low, as expected for zeolites without structural modification. After alkaline treatment with NaOH (Y-0.20), the BET surface area decreased by 25%, which can be attributed to a slight loss of crystallinity and partial collapse of the microporous network. However, a significant increase in mesopore volume was observed (from 0.163 to 0.380 $cm^3$ $g^{-1}$), along with an increase in the average pore diameter (from 59.5 to 82.4 Å), confirming the formation of wider secondary pores induced by the desilication process. This behaviour is indicative of effective structural hierarchization, in which part of the microporous system is replaced by mesopores, while largely preserving the structural integrity of the faujasite framework.[31,32]

In the composite catalysts, a clear dependence of the textural properties on both the type of zeolite used and its proportion in the formulation was observed. The catalysts are denoted as C30Y0.00, C30Y0.20, C40Y0.00, and C40Y0.20, where C refers to the zeolite loading (30 or 40 wt%) and Y indicates the NaOH concentration used during alkaline treatment (0.00 or 0.20 M). Catalysts formulated with hierarchical zeolite (C30Y0.20 and C40Y0.20) exhibited higher mesopore vol-umes (0.386 and 0.402 $cm^3$ $g^{-1}$, respectively) and larger average pore diameters (ranging from 97 to 99 Å) compared to their counterparts prepared with untreated zeolite (C30Y0.00 and C40Y0.00), whose mesopore volumes did not exceed 0.233 $cm^3$ $g^{-1}$. Moreover, increasing the zeolite content in the formulation (30% *vs.* 40%) led to a rise in both total surface area and total pore volume, especially in the catalysts prepared with hierarchical zeolite. For instance, catalyst C40Y0.20 displayed the highest mesopore volume (0.402 $cm^3$ $g^{-1}$), the largest mesopore surface area (301 $m^2$ $g^{-1}$), and the greatest average pore diameter (99.5 Å), confirming that the incorporation of a higher amount of treated zeolite positively impacts the development of a bimodal pore network. In contrast, catalyst C30Y0.00 exhibited the lowest mesoporosity, attributed to its higher micropore fraction and lower active phase content. These findings highlight the effectiveness of alkaline treatment as a strategy to enhance diffusivity in FCC catalysts through the generation of additional mesopores that facilitate mass transport. The creation of a hierarchical structure within the zeolite, and its preservation after incorporation into the

**Table 2** Textural, structural, and acidic properties of hierarchical zeolite-based catalysts

| | Y-0.00 | Y-0.20 | C30Y.0.00 | C30Y0.20 | C40Y0.00 | C40Y0.20 |
|---|---|---|---|---|---|---|
| BET specific surface area, $S_{BET}$ ($m^2$ $g^{-1}$) | 718 | 541 | 396 | 367 | 448 | 402 |
| Mesopore-specific surface area, $S_{meso}$ ($m^2$ $g^{-1}$) | 139 | 262 | 193 | 286 | 232 | 301 |
| Total pore volume, $V_{TP}$ ($cm^3$ $g^{-1}$) | 0.544 | 0.627 | 0.512 | 0.574 | 0.528 | 0.592 |
| Micropore volume, $V_{micro}$ ($cm^3$ $g^{-1}$) | 0.381 | 0.247 | 0.314 | 0.188 | 0.295 | 0.190 |
| Mesopore volume, $V_{meso}$ ($cm^3$ $g^{-1}$) | 0.163 | 0.380 | 0.198 | 0.386 | 0.233 | 0.402 |
| Average mesopore diameter, $\overline{d}_p$ (Å) | 59.5 | 82.4 | 69.2 | 97.4 | 74.6 | 99.5 |
| **Crystalline properties** | | | | | | |
| Crystallinity (%) | 99 | 68 | — | — | — | — |
| Unit cell size (Å) | 22.28 | 22.25 | — | — | — | — |
| **Acidic properties** | | | | | | |
| Brønsted acidity | | | | | | |
| Total (μmol Py $g^{-1}$) | 190 | 172 | 144 | 136 | 159 | 155 |
| Strong (%) | 30 | 36 | 28 | 34 | 29 | 35 |
| Lewis acidity | | | | | | |
| Total (μmol Py $g^{-1}$) | 66 | 70 | 52 | 60 | 58 | 64 |
| Strong (%) | 31 | 33 | 28 | 30 | 30 | 31 |

composite catalyst, represents a significant advancement in the design of catalysts with improved resistance to deactivation by coke and nitrogen-containing compounds, by improving access to active sites.

The acidity of the zeolites and composite catalysts was evaluated by pyridine adsorption coupled with infrared spectroscopy (pyridine-FTIR), using programmed thermal desorptions at 150 °C, 300 °C, and 400 °C. This technique, widely employed in heterogeneous catalysis, allows for quantification of the total acidity and differentiation between Brønsted and Lewis acid sites. Additionally, based on the desorption temperature, acid sites can be classified according to their relative strength (weak, medium, and strong), providing a comprehensive assessment of the acidic character of the materials.[33] In Table 2, in addition to the textural and structural properties, the total density of Brønsted and Lewis acid sites is reported, expressed in μmol of pyridine per gram of sample. Furthermore, the relative percentage of strong acid sites for each type is included, based on the amount of pyridine retained after desorption at 450 °C.

The zeolite base Y-0.00 exhibited the highest concentration of total acid sites, with a clear predominance of Brønsted-type centers, reflecting its high density of structural Si–OH–Al groups characteristic of the faujasite framework. In contrast, the hierarchical Y zeolite 0.20 showed a slight decrease in total acidity, attributed to the partial extraction of silicon and aluminum atoms during the alkaline desilication treatment. This modification led to an approximate 10% reduction in the density of Brønsted sites; however, a relative increase in the proportion of Lewis sites was observed, likely associated with structural defects or extra-framework species generated during the modification process. Despite the decrease in Brønsted site density, zeolite Y-0.20 exhibited a higher proportion of strong acid sites (retained after desorption at 450 °C), indicating greater thermal stability of the acid centers generated by the hierarchical structuring. This feature, combined with the previously observed increase in mesoporosity, could enhance catalytic activity under severe reaction conditions by improving both cracking efficiency and molecular access to active sites.

In the composite catalysts, a clear influence of both the zeolite type and content on the total acidity was observed. Materials with a higher zeolite loading (C40Y0.00 and C40Y0.20) exhibited higher total acid site densities compared to their 30% counterparts, reflecting the direct contribution of the active phase to the overall acidity of the system. Regarding the zeolite type, catalysts formulated with hierarchical zeolite (C30Y0.20 and C40Y0.20) showed lower total Brønsted acidity than their counterparts based on unmodified zeolite, a result consistent with the partial removal of Si–OH–Al groups induced by the alkaline desilication treatment. However, a higher relative proportion of Lewis sites was detected, likely associated with structural defects or extra-framework species generated during the modification process. A noteworthy observation is that the hierarchical catalysts retained a significant fraction of their acidity after desorption at 450 °C, indicating a greater proportion of thermally stable strong acid sites. These findings confirm that, although alkaline treatment reduces the total density of Brønsted sites, it promotes the generation of stronger acid centers. This redistribution in the nature and strength of acid sites is critical for catalytic performance in the presence of nitrogen containing com-pounds, as it enables the maintenance of reasonable activity under severe reaction conditions while reducing the catalysts susceptibility to deactivation by strong bases.

### 2.3. Catalytic activity

**2.3.1. Catalytic activity in the cracking of base VGO.** The catalytic performance was evaluated using Colombian vacuum gas oil (VGO) as a model feedstock, with the aim of comparing the intrinsic activity of the catalysts and analyzing their efficiency in terms of overall conversion and product selectivity. Fig. 2 presents the total VGO conversion results along with the distribution of products into three representative fractions: light gases (C1–C4), gasoline (C5–C12), and coke. Additionally, Table 3 summarizes both the product selectivity and the detailed composition of the gasoline fraction obtained during VGO cracking. The combined analyzis of conversion and product distribution enables a comprehensive evaluation of each catalysts performance, not only in terms of activity but also with regard to the quality and selectivity of the resulting fractions.[34] In particular, the gasoline composition provides critical insights into the potential octane rating and fuel quality, while coke yield serves as an indicator of catalyst stability and resistance to deactivation.

Catalysts formulated with a higher zeolite content (40 wt%) exhibited higher VGO conversion compared to those with a lower amount of active phase. This behaviour is attributed to the greater density of acid sites available to promote cracking reactions. In particular, the Cat40Y0.00 catalyst formulated with unmodified zeolite achieved the highest conversion among all tested materials, reaching a maximum value of 79 wt% at short residence times (20 s), reflecting its high total acidity, especially of Brønsted nature. However, this catalyst

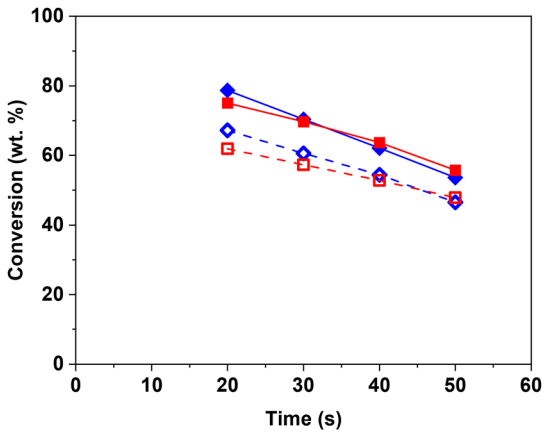


Fig. 2 Base VGO conversion at 550 °C as a reaction time function over catalysts. Symbols: diamonds, C40Y.0.00; open diamonds, C30Y0.00; squares, C40Y0.20; open squares, C30Y0.20.

Table 3 Product distribution (selectivities, wt%) and gasoline composition for VGO conversion at 550 °C (62 wt% conversion)

| Selectivities (wt%) | C30Y0.00 | C30Y0.20 | C40Y.0.00 | C40Y.0.20 |
|---|---|---|---|---|
| $S_{DG}$ | 15.4 | 12.4 | 17.1 | 10.7 |
| $S_{LPG}$ | 23.9 | 22.2 | 19.6 | 20.5 |
| $S_{GASOLINE}$ | 52.3 | 58.7 | 54.1 | 63.2 |
| **Gasoline composition (%)** | | | | |
| Paraffins | 25.3 | 24.0 | 21.9 | 22.9 |
| Olefins | 21.5 | 22.8 | 21.5 | 22.3 |
| Naphthenes | 19.1 | 15.9 | 20.4 | 14.4 |
| Aromatics | 34.1 | 37.3 | 36.2 | 40.4 |
| RON | 80.2 | 83.4 | 81.4 | 86.8 |
| $S_{COKE}$ (wt%) | 8.4 | 6.7 | 9.2 | 5.6 |

also showed a marked tendency toward coke formation, with yields increasing progressively as contact time increased. This behaviour suggests an enhanced formation of polyaromatic species and highly condensed products precursors of coke possibly resulting from diffusion limitations imposed by its predominantly microporous structure. Although the high acidity of the catalyst favours greater conversion at short contact times, this beneficial effect is offset by accelerated coke formation associated with intracrystalline diffusion constraints. This phenomenon negatively impacts catalytic stability, as the rapid pore blockage restricts access of reactive molecules to active sites, leading to faster deactivation.[35] As shown in Fig. 2, this deactivation manifests as a substantial drop in conversion at reaction times beyond 30 s, with conversion losses exceeding 25 wt%.

In contrast, the Cat40Y0.20 catalyst formulated with hierarchical zeolite exhibited a more stable conversion profile over the entire reaction time. Although its initial conversion was slightly lower, at contact times above 20 s (the typical range in industrial FCC units), this catalyst outperformed all others. This behaviour is attributed to the lower coke deposition within its porous network, a direct result of the hierarchical structure induced by alkaline treatment. The presence of interconnected mesopores facilitated the diffusion of reactants and intermediates, reducing the accumulation of polyaromatic species and mitigating the blockage of active sites. As a result, Cat40Y0.20 demonstrated greater resistance to time on stream deactivation, maintaining high conversion levels and catalytic efficiency even under more severe conditions. These findings highlight the relevance of hierarchical design as an effective strategy to optimize the balance between initial activity and operational stability in FCC catalyst systems.

Regarding product distribution, expressed in terms of selectivity toward the different fractions (Table 3), the catalysts formulated with hierarchical zeolites exhibited the highest selectivity toward the gasoline range (C5–C12) and the lowest coke yields. This behaviour is attributed to the mesopores generated during the desilication treatment, which enhance not only the diffusion of reactant molecules but also the transport of intermediate and final products within the gasoline range. This improved molecular diffusion reduces secondary cracking reactions that typically lead to the formation of lighter, less valuable products (C1–C4), while simultaneously limiting the formation of coke. Overall, these results suggest that the hierarchization of Y zeolite provides a favourable balance between catalytic activity and product selectivity by minimizing coke deposition and promoting the formation of higher value fractions such as gasoline. In addition to textural effects, the nature and distribution of acid sites play a critical role in controlling product selectivity. Catalysts prepared with the Y0.00 zeolite, characterized by a higher density of Brønsted acid sites and a predominantly microporous structure, tend to increase the residence time of reactive intermediates within the catalyst. Under these conditions, bimolecular side reactions such as condensation and hydride transfer are favoured. Consequently, olefins and aromatics initially formed can act as precursors to heavier polyaromatic species, which progressively evolve into coke, thereby reducing their observed selectivity. Conversely, catalysts prepared with the Y0.20 zeolite, which exhibit a greater contribution of Lewis acid sites together with enhanced mesoporosity, favour less severe cracking pathways and faster desorption of olefins and aromatics. This combination limits the secondary transformation of these products into coke and explains the higher selectivity toward olefins and aromatics, as well as the lower coke yields observed for these catalysts. With respect to the zeolite content in the catalyst formulation, it was observed that increasing the zeolite loading from 30% to 40% led to higher VGO conversion and greater gasoline production, particularly in catalysts containing hierarchical zeolite. In particular, the C40Y0.20 catalyst exhibited the highest selectivity toward gasoline, reflecting a more efficient cracking performance.

Another important parameter in evaluating catalytic performance is the quality of the gasoline fraction, which was estimated by the research octane number (RON). As shown in Table 3, the RON values followed the trend: C30Y0.00 = 80.2, C40Y0.00 = 81.4, C30Y0.20 = 83.4, and C40Y0.20 = 86.8, with the latter catalyst generating the highest-quality gasoline. This variation in RON correlates directly with the chemical composition of the gasoline cut. Specifically, the C40Y0.20 catalyst, formulated with a higher proportion of hierarchical zeolite, promoted a greater formation of aromatics and olefins, compounds with high anti-knock properties that contribute significantly to octane enhancement. In contrast, the gasoline produced by the C30Y0.00 catalyst contained a higher proportion of paraffins, which are associated with lower RON values, resulting in a less desirable fuel fraction.

These findings reinforce the positive impact of Y zeolite hierarchization not only in enhancing diffusivity and selectivity toward valuable products but also in optimizing the quality of the liquid fuel obtained, a key consideration for commercial FCC catalyst applications. Moreover, this beneficial effect is further amplified by increasing the zeolite content, highlighting a synergistic interaction between intramolecular mesoporosity and acid site availability. In this synergistic system, the increased density of accessible active sites combined with enhanced diffusion pathways promotes higher selectivity toward olefins and aromatics, improves gasoline quality, and effectively suppresses coke formation.

### 2.3.2. Impact of nitrogen-containing compounds on catalyst performance

*2.3.2.1. Conversion.* The presence of nitrogen-containing compounds in feedstocks is one of the most critical causes of catalytic deactivation in fluid catalytic cracking (FCC) processes, due to their strong affinity for Brønsted acid sites within the zeolite structure. These basic species compete directly with hydrocarbon molecules for access to active sites, which can negatively impact both VGO conversion and product distribution, as well as overall catalyst stability. In this study, the effect of two model organic nitrogen compounds (quinoline and indole) was investigated. Both exhibit heterocyclic aromatic structures but differ significantly in basicity. The individual and combined effects of these compounds on the conversion of VGO were evaluated using the four FCC catalysts formulated with different Y zeolite contents (30 wt% and 40 wt%) and levels of hierarchical structuring. Fig. 3 shows the conversion profiles of the different feedstocks over the composite catalysts at 550 °C. Specifically, the plots illustrate the conversion behaviour of VGO doped with quinoline alone (Fig. 3a), with indole alone (Fig. 3b), and with both compounds simultaneously (Fig. 3c). The results reveal a significant reduction in conversion in the presence of nitrogen-containing compounds, with quinoline having the strongest inhibitory effect. This difference is attributed to its higher basicity ($pK_a \approx 4.9$), which promotes stronger and more competitive adsorption onto Brønsted acid sites, compared to indole ($pK_a \approx -2.4$), whose interaction is weaker and partially reversible at reaction temperatures.

Comparatively, the catalysts formulated with hierarchical zeolite (Y-0.20) exhibited smaller losses in conversion relative to their conventional counterparts (Y-0.00). This improved performance is attributed to the higher presence of mesopores in the hierarchical systems, which facilitates internal diffusion, reduces local accumulation of strongly basic species, and promotes the desorption of partially protonated nitrogen compounds, thereby shortening their residence time within the catalytic matrix. In all cases, the drop in conversion was more severe for catalysts containing only 30 wt% zeolite, due to their lower overall density of active sites and greater susceptibility to site neutralization by basic contaminants. As expected, the simultaneous presence of both quinoline and indole in the VGO03 feedstock had the most detrimental effect, with conversion values dropping to approximately 30 wt%. This negative impact was particularly pronounced for the Cat30Y0.00 catalyst, which exhibited the highest loss of activity when processing the quinoline-doped feed, confirming the need for hierarchical structures and higher zeolite loadings to mitigate deactivation under nitrogen rich conditions.

These results underscore the importance of designing catalysts with optimized textural properties and a well-balanced acid site distribution to maintain catalytic activity even under severe conditions associated with contaminated feedstocks such as those derived from heavier or less treated crude fractions.

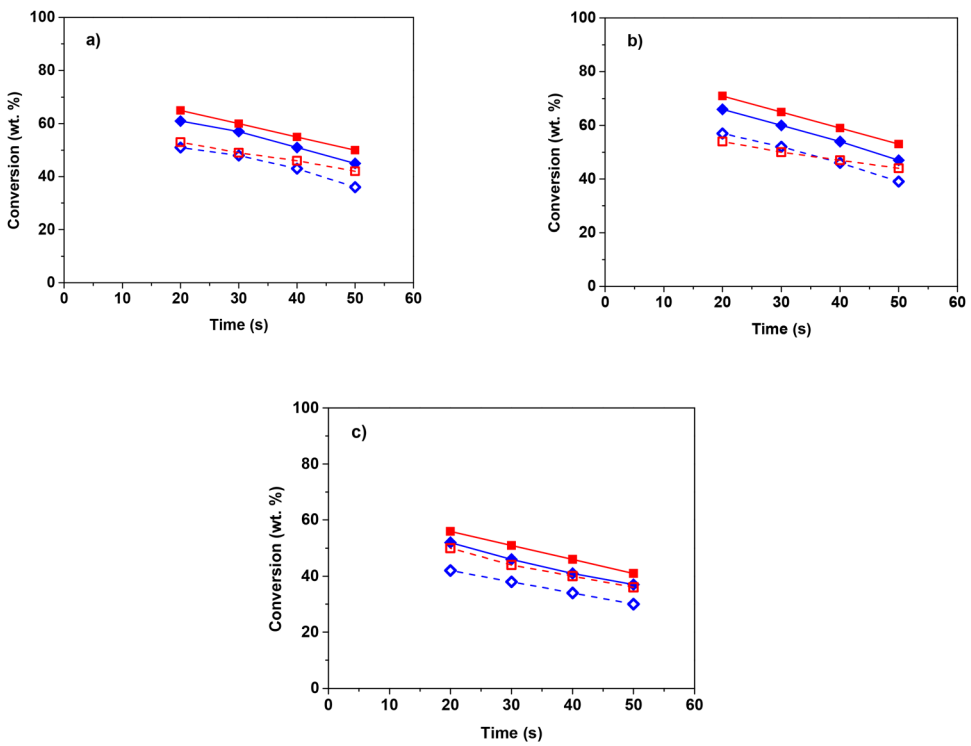


Fig. 3 Conversion of nitrogen-doped VGO feedstocks at 550 °C as a function of reaction time over FCC composite catalysts. Feedstocks: (a) VGO01 (quinoline), (b) VGO02 (indole), and (c) VGO03 (quinoline + indole). Symbols: diamonds, C40Y.0.00; open diamonds, C30Y0.00; squares, C40Y0.20; open squares, C30Y0.20.

*2.3.2.2. Product distribution.* The presence of nitrogenous bases in the feed disrupts the accessibility and availability of the catalyst's acid sites, thereby affecting the product distribution. This section analyzes the evolution of the main product fractions gases, gasoline, and coke upon the individual and combined addition of quinoline and indole to the VGO feedstock, taking into account the influence of both zeolite type and loading in each catalyst formulation. As previously discussed, under contaminant-free conditions, the hierarchical catalysts with higher zeolite content (C40Y0.20) exhibited the highest selectivity toward gasoline. However, the addition of quinoline led to a systematic decrease in gasoline yield across all catalysts, particularly in the conventional formulations (C30Y0.00 and C40Y0.00), accompanied by a proportional increase in coke formation. The selectivities of the various product fractions, as well as the composition and quality of the gasoline cut, are summarized in Table 4. This shift toward coke is directly associated with the inhibition of β-scission, cyclization, and deprotonation mechanisms typically promoted by Brønsted acid sites which are occupied or neutralized by quinoline. In contrast, the addition of indole had a less severe effect on product distribution (see Table 5). This behaviour reflects the lower basicity of indole, making it a less aggressive contaminant and allowing for the persistence of catalytic activity associated with medium and strong-acidity sites. As a result, the hierarchical catalysts retained a higher proportion of the desired products, even in the presence of indole.

Additionally, an increase in the production of light gases (mainly $C_3$–$C_4$) was observed in the presence of quinoline, which is attributed to non-selective secondary cracking pathways promoted under conditions of residual acidity. On the other hand, the quality of the gasoline fraction, assessed *via* the research octane number (RON), was adversely affected by the presence of nitrogen compounds. The neutralization of Brønsted acid sites limits the formation of branched olefins and light aromatics key components for achieving high RON values. In this context, hierarchical catalysts with improved pore accessibility were able to partially preserve gasoline quality, as evidenced by a higher proportion of olefins and light aromatics (C7–C9), which are crucial for achieving estimated RON values above 80. A noteworthy observation is that the hierarchical catalysts (Y-0.20) exhibited lower coke accumulation even under nitrogen contaminated conditions. This suggests that the introduction of mesoporosity contributes not only to enhanced diffusion of reactants and products, but also to reduced retention of nitrogenated aromatic species, which are key precursors in coke formation. This effect is most evident in catalyst C40Y0.20, whose optimized balance of pore accessibility, acidity, and resistance to poisoning allows it to maintain a favourable product distribution. Overall, the results indicate that both zeolite hierarchization and increased zeolite content are effective strategies to mitigate the negative impact of nitrogen contaminants. The observed product redistribution in their presence can be interpreted as a direct consequence of the selective neutralization of the most catalytically relevant active sites for gasoline and light gas formation. This loss in selectivity can be partially offset through structural designs that promote diffusional transport and acidity redistribution within the catalyst matrix. Other strategies for improving the catalytic performance of zeolites under FCC conditions have been described in the literature. For example, Han *et al.*[36] investigated the synergistic modification of ZSM-5 with tungsten and phosphorus for heavy oil cracking, demonstrating that the improvement in catalytic performance was closely related to better preservation of acid sites and greater hydrothermal stability. In this system, the interaction between the W and P species played a key role in mitigating deactivation and maintaining product selectivity.

Unlike these metal and phosphorus based modifications, the present study demonstrates that comparable mitigation of nitrogen-induced deactivation and coke formation can be achieved through a purely structural approach based on the introduction of hierarchical porosity. The improved accessibility and diffusional transport provided by hierarchical zeolites promote more efficient utilization of the remaining active sites, thus preserving a favourable product distribution even under nitrogen-contaminated conditions.

The simultaneous evaluation of the effects of quinoline and indole during the catalytic cracking of VGO provides a more realistic approximation of the conditions encountered in nitrogen contaminated feedstocks, where basic and neutral compounds commonly coexist and compete for active sites. A markedly more severe impact was observed when both quino-

**Table 4** Product distribution (selectivities, wt%) and gasoline composition for VGO01 conversion at 550 °C (62 wt% conversion)

| Selectivities (wt%) | C30Y0.00 | C30Y0.20 | C40Y.0.00 | C40Y.0.20 |
|---|---|---|---|---|
| $S_{DG}$ | 17.2 | 13.9 | 17.7 | 10.9 |
| $S_{LPG}$ | 25.9 | 25.0 | 20.4 | 23.1 |
| $S_{GASOLINE}$ | 47.1 | 53.2 | 51.7 | 58.8 |
| **Gasoline composition (%)** | | | | |
| Paraffins | 22.0 | 25.1 | 23.4 | 22.9 |
| Olefins | 20.2 | 20.5 | 19.2 | 22.7 |
| Naphthenes | 25.1 | 18.4 | 23.1 | 15.9 |
| Aromatics | 32.7 | 36.0 | 34.3 | 38.5 |
| RON | 78.1 | 80.9 | 79.5 | 83.4 |
| $S_{COKE}$ (wt%) | 9.8 | 7.9 | 10.2 | 7.2 |

**Table 5** Product distribution (selectivities, wt%) and gasoline composition for VGO02 conversion at 550 °C (62 wt% conversion)

| Selectivities (wt%) | C30Y0.00 | C30Y0.20 | C40Y.0.00 | C40Y.0.20 |
|---|---|---|---|---|
| $S_{DG}$ | 16.3 | 14.4 | 14.7 | 11.6 |
| $S_{LPG}$ | 24.9 | 22.1 | 22.6 | 20.8 |
| $S_{GASOLINE}$ | 50.8 | 56.2 | 53.1 | 61.3 |
| **Gasoline composition (%)** | | | | |
| Paraffins | 20.2 | 19.3 | 21.0 | 18.9 |
| Olefins | 21.5 | 21.6 | 20.6 | 23.5 |
| Naphthenes | 24.4 | 20.6 | 22.3 | 17.2 |
| Aromatics | 33.9 | 38.5 | 36.1 | 40.4 |
| RON | 79.8 | 82.3 | 82.4 | 85.2 |
| $S_{COKE}$ (wt%) | 8.0 | 7.3 | 9.6 | 6.3 |

line and indole were introduced together into the feedstock (see Table 6). Under this scenario, a further decline in gasoline and light gas yields was recorded, accompanied by a significant increase in coke formation surpassing the effects produced by each compound individually. This synergistic deactivation can be attributed to the complementary interaction of both nitrogen species with different types of acid sites: while quinoline preferentially targets the stronger Brønsted sites, indole may additionally interfere with weaker acid centers or serve as a precursor for heavier aromatic intermediates. The concurrent presence of both contaminants leads to more extensive coverage of the active surface, suppressing key cracking pathways such as β-scission and promoting secondary condensation reactions that drive coke generation.

In addition, a deterioration in the quality of the gasoline fraction was evident, characterized by a lower olefin/paraffin ratio and reduced content of C7–C9 hydrocarbons molecules that typically enhance the octane number. Despite this highly unfavourable context, the hierarchical catalysts retained superior performance, with C40Y0.20 once again demonstrating the lowest yield loss and strongest resistance to coke buildup. These findings highlight the critical importance of hierarchical pore design and optimized acidity distribution for preserving catalytic functionality under chemically aggressive environments containing complex nitrogen species.

*2.3.2.3. Deactivation resistance: nature of coke.* Catalyst resistance to deactivation was evaluated through temperature programmed oxidation (TPO) analyzis of the deposited coke, with the resulting profiles shown in Fig. 4. The formation, type, and combustibility of coke were directly influenced by both the nature of the catalyst and the presence of nitrogen containing compounds in the feedstock. Under nitrogen free conditions (base VGO, Fig. 4a), all catalysts exhibited two well-defined thermal signals: a minor peak below 450 °C, attributed to light coke more reactive and richer in aliphatic chains and a dominant peak above 535 °C, corresponding to dense aromatic coke, structurally more complex and thermally resistant. The relative intensity and position of this second peak varied depending on the type and concentration of zeolite in the catalyst. In particular, catalysts formulated with conventional zeolites (C40Y0.00 and C30Y0.00) showed stronger peak shifts toward higher temperatures (up to 570 °C), suggesting the accumulation of more condensed coke, strongly anchored within confined or less accessible acid sites.

Upon introducing basic nitrogen compounds, significant changes were observed in both the amount and nature of the coke formed (Fig. 4b–d). For the VGO01 feed (Fig. 4b), doped with quinoline, the main oxidation peak for the C40Y0.00 catalyst shifted up to 585 °C, indicating a greater resistance to combustion. This shift can be attributed to the strong competitive adsorption of quinoline on Brønsted acid sites, which disrupts cracking pathways and promotes polycondensation and aromatization reactions, leading to denser, more stable coke. Furthermore, partial neutralization of the catalyst acidity reduces the desorption of heavy intermediates, increasing their residence time and favouring their transformation into carbonaceous species resistant to oxidation. For the VGO02 feedstock (Fig. 4c), doped with indole, the effect was less pronounced. Although thermal shifts were observed, they were more moderate (up to 574 °C for C40Y0.00), consistent with the lower basicity of indole compared to quinoline. This suggests weaker interaction with acid sites and, consequently, a reduced contribution to the formation of highly condensed coke. The VGO03 feed (Fig. 4d), doped with a mixture of quinoline and indole, exhibited the most severe TPO shifts, with maximum oxidation temperatures exceeding 590 °C in conventional catalysts. This behaviour indicates negative synergies between the two nitrogen compounds, promoting coalescence of aromatic precursors and enhanced thermal stability of the coke. The higher peak intensities and temperature shifts observed in the TPO profiles reflect not only a greater total coke content but also reduced accessibility of molecular oxygen to the internal zones where coke was deposited likely due to pore blockage by condensed nitrogenous species. These findings are corroborated by the post-reaction textural analyzis of the coked catalysts, which is discussed in Section 2.3.2.4.

In comparison, catalysts formulated with hierarchical zeolite (C30Y0.20 and C40Y0.20) consistently exhibited less severe TPO profiles across all feedstocks, both in terms of peak position and intensity. This difference can be attributed to the presence of intracrystalline mesopores, which enhance the diffusion of reactants and products, allow more efficient desorption of intermediates, and reduce the likelihood of transformation into structured coke. Furthermore, the more accessible and less confined distribution of acid sites in hierarchical zeolites prevents the formation of strongly anchored carbon deposits. From an operational perspective, these observations have critical implications for FCC processes. The formation of denser, more refractory coke not only diminishes catalytic activity but also hampers regeneration by requiring higher temperatures and longer times. This may compromise the thermal efficiency of the regenerator and accelerate irreversible deactivation through sintering or poisoning. Conversely, hierarchical catalysts not only generate lower amounts of coke but also produce deposits that are more easily oxidized, thus enabling faster, more sustainable, and energy efficient regeneration cycles. Other studies reported in the literature have investigated the deactivation of catalysts by coke deposition using

**Table 6** Product distribution (selectivities, wt%) and gasoline composition for VGO03 conversion at 550 °C (62 wt% conversion)

| Selectivities (wt%) | C30Y0.00 | C30Y0.20 | C40Y.0.00 | C40Y.0.20 |
|---|---|---|---|---|
| $S_{DG}$ | 20.4 | 17.9 | 19.6 | 12.8 |
| $S_{LPG}$ | 20.6 | 23.3 | 18.3 | 24.4 |
| $S_{GASOLINE}$ | 44.4 | 49.7 | 48.3 | 53.4 |
| **Gasoline composition (%)** | | | | |
| Paraffins | 27.2 | 27.7 | 25.8 | 23.0 |
| Olefins | 18.7 | 19.5 | 19.4 | 21.3 |
| Naphthenes | 24.5 | 19.9 | 23.3 | 20.1 |
| Aromatics | 29.6 | 32.9 | 31.5 | 35.6 |
| RON | 75.2 | 77.6 | 76.1 | 80.2 |
| $S_{COKE}$ (wt%) | 14.6 | 9.1 | 13.8 | 9.4 |

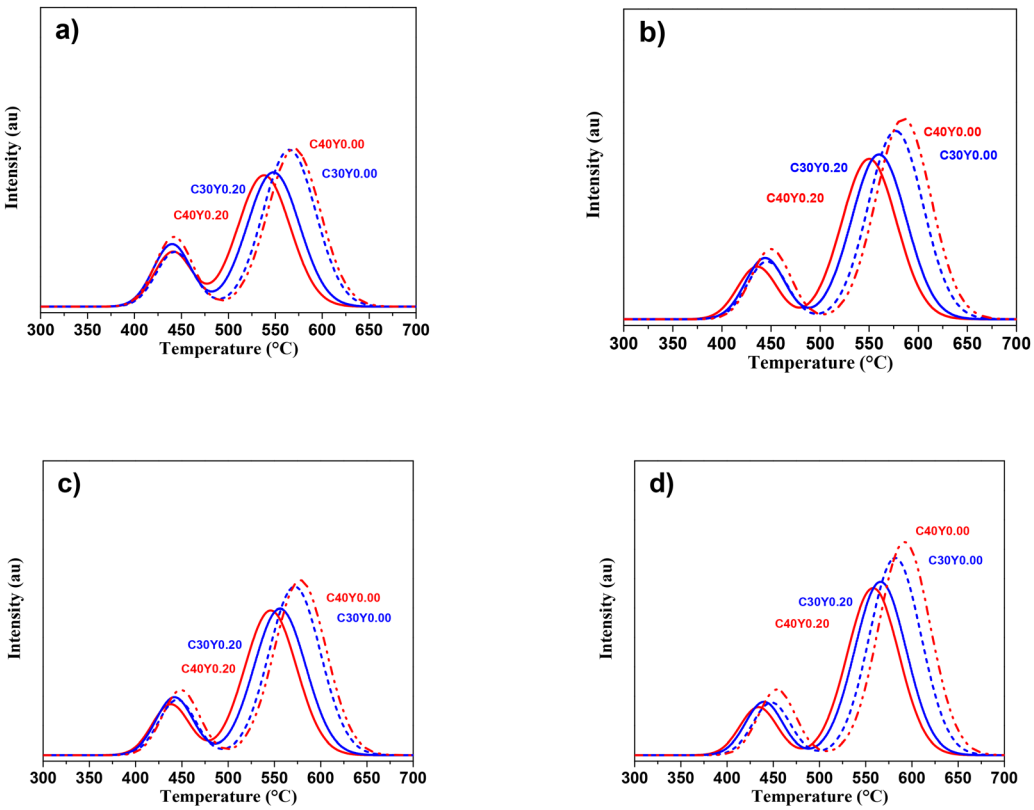


**Fig. 4** TPO profiles of coke deposited on spent catalysts after VGO conversion (~62 wt%). Feedstocks: (a) base VGO, (b) VGO01 (quinoline), (c) VGO02 (indole), and (d) VGO03 (quinoline + indole).

bimetallic catalytic systems. While these approaches have been primarily investigated in reaction environments other than FCC, such as dry methane reforming, they provide valuable information on the mechanisms of coke formation and removal. In these systems, bimetallic catalysts exhibit greater resistance to deactivation due to synergistic metal–metal interactions, which modify the structure, growth, and combustibility of the carbonaceous deposits, thereby improving the catalyst's stability and regenerability.[37]

*2.3.2.4. Impact of coke deposition on catalyst properties.* To evaluate the resistance of the catalysts to deactivation under conditions representative of industrial catalytic cracking processes, the evolution of their textural and acidic properties was analyzed after the conversion of VGO, both in the absence and presence of nitrogen-containing compounds (quinoline and indole). Textural properties were assessed by nitrogen physisorption, while acidity was evaluated *via* pyridine ad-sorption followed by FTIR spectroscopy at different desorption temperatures. This characterization enabled the identification of structural changes, pore blockage, and loss of active sites as a consequence of coke deposition and chemical interaction with basic contaminants.

Textural Changes Induced by Coke Deposition. Fig. 5 shows the changes in textural properties observed after catalytic cracking. In all cases, a significant reduction in specific surface area and average mesopore diameter (calculated by the

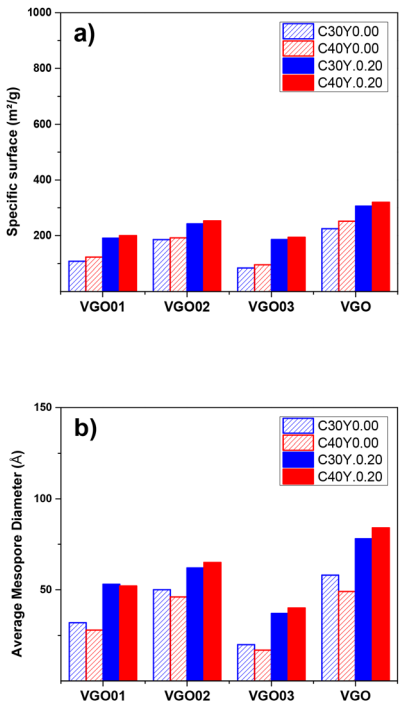


**Fig. 5** Textural properties of spent FCC catalysts after sVGO cracking. (a) BET surface area; (b) average mesopore diameter. Feedstocks: base VGO, VGO01 (quinoline), VGO02 (indole), and VGO03 (quinoline + indole).

BJH method) was observed, suggesting partial blockage of the porous structure due to coke formation. The decrease in surface area was more pronounced in catalysts formulated with conventional zeolite (C30Y0.00 and C40Y0.00), with losses exceeding 70%, whereas in catalysts con-training hierarchical zeolites (C30Y0.20 and C40Y0.20), the reduction was less severe, not surpassing 50%. This greater textural stability in hierarchical catalysts suggests that the introduction of additional mesopores facilitates the diffusion of heavy molecules, thereby reducing coke accumulation within the zeolite crystals and mitigating structural collapse. The presence of a hierarchical pore network acts as a diffusion pathway for bulky inter-mediates and products, limiting the formation of recalcitrant carbonaceous species in critical regions of the catalyst.

Acid site deactivation: influence of coke and nitrogen contaminants. A significant loss in total surface acidity was also observed after cracking, particularly in the presence of nitrogen-containing compounds. Fig. 6 shows the relationship between acidity loss and coke yield for each feedstock. The most severe Brønsted acid site deactivation per unit mass of coke occurred in catalysts exposed to VGO03 (doped with both quinoline and in-dole), followed by VGO01 (quinoline only), and finally the base VGO. This trend reflects the ability of basic compounds to selectively neutralize Brønsted acid sites, acting as direct catalytic poisons even before inducing significant coke formation. Quinoline, being more basic than indole, exhibited a stronger affinity for the protons of Brønsted sites,

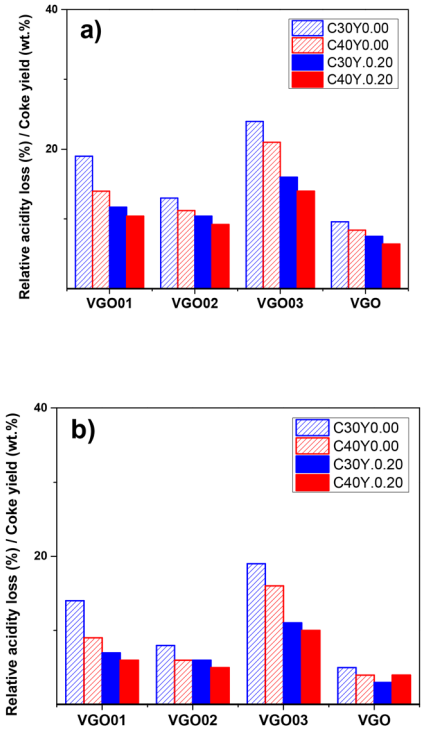


Fig. 6 Relative acidity loss (%) per unit of coke yield (wt%) in spent FCC catalysts. (a) Brønsted acid sites; (b) Lewis acid sites. Feedstocks: base VGO, VGO01 (quinoline), VGO02 (indole), and VGO03 (quinoline + indole).

resulting in more pronounced acid loss. In contrast, Lewis acid sites were less affected, indicating greater resistance to direct chemical deactivation. Additionally, the presence of these nitrogen species favoured the formation of more condensed, harder-to-remove coke, which contributed to irreversible pore blockage and exacerbated the loss of textural properties especially in catalysts containing 30 wt% conventional zeolites. In the absence of nitrogen contaminants, all catalysts experienced a moderate reduction in acidity, primarily attributable to the coverage of active sites by light coke and superficial thermal effects. However, catalysts containing hierarchical zeolite preserved a higher proportion of active acid sites, both Brønsted and Lewis. Specifically, Brønsted acidity loss in hierarchical catalysts ranged from 20% to 30%, while in non-hierarchical counterparts it exceeded 40%, confirming their greater structural and chemical vulnerability.

The results obtained allow for the establishment of a clear correlation between catalyst design, structural stability, and resistance to acid site deactivation induced by coke. Among all materials, the hierarchical catalysts with higher active phase content (particularly C40Y0.20) exhibited the best overall performance, preserving both porosity and a higher proportion of functional acidity even under severe cracking conditions involving nitrogen contaminants. This synergy between hierarchical structuring and high zeolite loading not only enhances access to catalytic sites during the reaction but also limits the formation of obstructive coke and mitigates the extent of chemical deactivation. Taken together, these findings reaffirm that coke deposition and the presence of basic compounds significantly compromise catalytic functionality, affecting both structural integrity and acid site availability. However, by adopting a design strategy that incorporates additional mesoporosity and an optimized active phase content, it is possible to substantially im-prove the resilience of FCC catalysts against typical deactivation mechanisms encountered during the processing of nitrogen-rich heavy feedstocks.

**2.3.3. Implications for industrial catalyst design.** The findings of this study highlight the relevance of hierarchical Y zeolite design as an effective strategy to enhance both the activity and stability of FCC catalysts under conditions representative of nitrogen-contaminated heavy crudes, particularly those typical of Latin American sources. Specifically, the incorporation of mesoporosity through controlled alkaline treatments significantly improved the accessibility of reactive molecules to acid sites, mitigating deactivation caused by diffusional limitations and facilitating the preservation of Brønsted acidity in the presence of strongly basic species such as quinoline. The superior performance observed in catalysts containing 40 wt% hierarchical zeolite suggests that a higher active phase content when hierarchically structured—not only enhances VGO conversion but also improves gasoline selectivity and reduces coke formation, without compromising structural stability or residual acidity. This evidence sup-ports the formulation of hierarchical FCC catalysts with optimized Y zeolite content as a robust pathway to improve industrial performance in FCC units processing nitrogen-rich heavy feeds,

without the need for costly pretreatment steps or harsh operating conditions.

Nevertheless, certain limitations of this study must be acknowledged, such as the absence of regeneration cycles and the use of model nitrogen compounds instead of more representative industrial mixtures. Therefore, future research should incorporate regeneration tests, experiments under fluidized-bed or pilot plant conditions, and extended characterization of catalyst behaviour under continuous exposure to contaminants. These developments will help advance toward the design of more robust and selective formulations, tailored to the real-world operational challenges of the Latin American refining industry.

# 3. Materials and methods

Catalytic conversion experiments were conducted in a fixed-bed reactor (MAT unit) using four different feedstocks and four FCC-type catalysts. The feedstocks consisted of vacuum gas oils (VGOs) containing varying concentrations of nitrogen-containing compounds. The catalysts employed were formulated with typical fluid catalytic cracking (FCC) compositions, containing either 30 wt% or 40 wt% zeolite. The catalysts were identified as C30Y0.00, C30Y0.20, C40Y0.00, and C40Y0.20. The number associated with the letter C represents the zeolite content (weight percent) incorporated during the catalyst preparation (30 or 40 weight percent), while the subscript Y indicates the concentration of sodium hydroxide used in the alkaline treatment of the zeolite, with Y0.00 being the untreated sample and Y0.20 the sample treated with 0.20 M NaOH.

## 3.1. Feedstock production and nitrogen doping

The VGOs used in this study were obtained at laboratory scale from Colombian crude oils through a two-stage distillation process, adapted from the ASTM D2892-18 standard.[38] In the first stage, an atmospheric distillation was performed by heating the crude oil at a rate of 10 °C $min^{-1}$ up to 220 °C to recover straight-run naphtha. After maintaining this temperature for 30 minutes, heating was resumed at the same rate until reaching 370 °C to collect the straight-run gas oil, leaving behind the atmospheric residue in the distillation flask. This residue was subsequently cooled to 220 °C for the second stage, which involved vacuum distillation. The vacuum distillation was carried out with a heating rate of 5 °C $min^{-1}$ from 220 °C to 370 °C, maintaining the final temperature for 30 minutes to obtain the vacuum gas oil and vacuum residue.

The VGO obtained was characterized and subsequently doped with model nitrogen-containing compounds to simulate high concentrations of nitrogen contaminants in the feed and assess their impact on catalyst deactivation. The base VGO initially contained 0.1 wt% nitrogen. From this material, three distinct feedstocks were prepared using representative nitrogen compounds: quinoline, a basic aromatic species, and indole, a neutral nitrogen compound.[39] Both are commonly found in typical Colombian refinery streams.[40,41] The first sample (VGO01) was enriched exclusively with quinoline to achieve a final nitrogen concentration of 0.5 wt% (0.4% from quinoline and 0.1% from the base VGO), by adding 3.65 g of quinoline to 100 mL of VGO. The second sample (VGO02) was doped solely with indole, also reaching a total nitrogen concentration of 0.5 wt% by adding 3.29 g of indole. A third sample (VGO03) was formulated to simulate more severe nitrogen contamination, incorporating both compounds, 3.48 g of quinoline and 3.16 g of indole, resulting in a total nitrogen content of 0.9 wt%.

In all cases, the doping process was performed under continuous magnetic stirring at 50 °C for 1 hour to ensure complete dissolution of the nitrogen compounds. This temperature was sufficient to promote full solubility in the heavy hydrocarbon matrix without the need for auxiliary solvents, as both quinoline and indole exhibit good solubility in VGO under mild thermal conditions.

## 3.2. Feedstocks characterization

The physicochemical characterization of the vacuum gas oil feedstocks was per-formed using standard analytical protocols to determine key properties influencing cata-lytic cracking performance. The density of each feedstock was expressed in terms of API gravity, measured according to the ASTM D287-12b method.[42] The carbon forming potential was assessed through determination of Conradson carbon residue (CCR) using the micro method specified in ASTM D4530-15.[43] Boiling range distributions were obtained by simulated distillation (SIMDIS) on a Shimadzu GC-2014 gas chromatograph equipped with a flame ionization detector (FID) and a non-polar capillary column (30 m length, 250 μm internal diameter, and 0.25 μm film thickness), following the ASTM D2887-23 standard.[44] This analysis provided detailed distillation profiles for each VGO sample.

The molecular composition of the feedstocks was evaluated through SARA fractionation separating saturates, aromatics, resins, and asphaltenes according to the ASTM D2007-11 procedure.[45] This technique allows for assessment of polarity and compositional complexity, which are key factors in determining cracking behaviour and catalyst interaction. Trace metal concentrations, including nickel (Ni), vanadium (V), sodium (Na), and iron (Fe), were quantified *via* inductively coupled plasma optical emission spectrometry (ICP-OES) using a PerkinElmer Optima 7300 DV instrument.[46] These metals are commonly associated with catalyst fouling and loss of activity in FCC processes. Total nitrogen content in the VGO samples was determined by elemental analysis to quantify the concentration of nitrogen-containing compounds,[47] which play a critical role in catalyst deactivation. This measurement served both to characterize the native feed and to verify the nitrogen enrichment achieved through model compound doping. The complete set of physicochemical properties for the VGOs is summarized in Table 1.

## 3.3. Alkaline treatment of Y zeolites

In this work, a commercial Y zeolite with a Si/Al ratio of 31 was used, which was modified by desilication in an alkaline

medium following a methodology previously re-ported by our group.[48] The treatment involved suspending 4 g of zeolite in 100 mL of 0.20 M NaOH, stirring for 15 minutes at room temperature. Subsequently, the mixture was neutralized with 1.00 M HCl to reach a pH of 2, followed by three ion-exchange cycles using 0.50 M $NH_4Cl$. After washing and filtering, both the original and treated samples were subjected to a hydrothermal stabilization process in a tubular steel reactor. In this step, 2 g of each sample were initially heated to 250 °C at a rate of 5 °C $min^{-1}$, and once the temperature stabilized, water vapor was fed at 1.0 g $min^{-1}$ while the temperature was increased to 780 °C at a rate of 10 °C $min^{-1}$. Both samples, referred to as Y-0.00 and Y-0.20, exhibited a weight recovery greater than 95% after treatment.

### 3.4. Catalyst synthesis

The hierarchical and original zeolites obtained in Section 3.3 were used to formulate fluid catalytic cracking (FCC) catalysts, following representative compositions of commercial systems. In these composite catalysts, the Brønsted acid sites associated with the Y zeolite act as the main active centers responsible for the catalytic cracking reaction, while the zeolite itself constitutes the active phase and the matrix components mainly contribute to dispersion and mass transport. Two formulations were prepared: one containing 30 wt% Y zeolite, 50 wt% matrix (silica–alumina and clay-based components), and 20 wt% binder; and another containing 40 wt% Y zeolite, 40 wt% matrix, and 20 wt% binder. Mesoporous silica (chromatographic grade), previously sieved (75–105 μm) and calcined at 550 °C, was used as the matrix. The zeolite and matrix were homogeneously mixed, while the binder was prepared from a suspension of colloidal silica (Ludox AS-40 at 40 wt%) and deionized water. This suspension was dried at 90 °C for 2 hours, ground, sieved (75–105 μm), and subsequently calcined at 550 °C for 4 hours. The resulting catalysts were designated as C30Y0.00, C30Y0.20, C40Y0.00, and C40Y0.20, depending on the type of zeolite used (Y-0.00 or Y-0.20) and its proportion in the formulation. The overall synthesis yield ranged from 90% to 95% by weight, based on the total dry mass of the starting components.

### 3.5. Catalysts characterization

A comprehensive physicochemical characterization was conducted on the four FCC catalyst formulations, in both their fresh and spent (coked) states, to assess differences in structural, textural, and acidic properties. The crystallographic structure was first examined using X-ray diffraction (XRD), employing a Siemens D500 diffractometer with a CuKα radiation source ($\lambda$ = 1.5418 Å).[49] Scans were conducted over a $2\theta$ range of 5–50° with a step size of 0.05° and a dwell time of 3 seconds per step. Crystallinity indices and unit cell dimensions were determined according to ASTM standards D3906-03 and D3942-19, respectively.[49,50] Textural analysis was carried out *via* nitrogen physisorption using a Micromeritics 3-Flex™ automated surface area analyzer.[51] Prior to measurement, the catalysts were degassed under high vacuum ($10^{-6}$ mmHg) at 300 °C for 24 hours to remove any physisorbed contaminants. Adsorption–desorption isotherms were collected at liquid nitrogen temperature (−196 °C). BET surface area was calculated from the isotherms, while total pore volume was estimated from nitrogen uptake at a relative pressure ($P/P_0$) of approximately 0.98. The Barrett–Joyner–Halenda (BJH) method was applied to derive meso-pore size distribution and average pore diameter. Micropore volume and mesopore surface area were further evaluated using the *t*-plot method. Acidity characterization was per-formed by Fourier transform infrared spectroscopy (FTIR) with pyridine as a probe molecule. Self-supported wafers (15 mm diameter, 80 mg) were prepared using 4 tons per $cm^2$ of compression.[52] Samples were degassed at 450 °C under vacuum ($10^{-3}$ Torr) for 2 hours, followed by acquisition of background spectra at room temperature. Pyridine adsorption was carried out at ambient temperature, and desorption was performed stepwise at 150, 300, and 400 °C to assess acid site strength. FTIR spectra were recorded using a Nicolet spectrophotometer at 4 $cm^{-1}$ resolution, with 256 scans per spectrum. The characteristic absorption bands at 1540 and 1450 $cm^{-1}$ were used to distinguish Brønsted and Lewis ac-id sites, respectively. The quantity of pyridine retained at 150 °C corresponds to the total acid site population, whereas retention at 300 °C and 400 °C represents medium-to-strong and strong acid sites, respectively. A summary of the structural and chemical properties of the catalysts is presented in Table 2.

The characterization of coke deposited on spent catalysts was performed using analytical techniques previously established in related studies, aimed at determining both the composition and spatial distribution of carbonaceous residues formed during the cracking reactions. To evaluate nature and quantify the amount of coke, temperature-programmed oxidation (TPO) was employed. In this method, the carbonaceous material was oxidized in a flow of nitrogen containing 1% oxygen (v/v), generating carbon monoxide (CO) and carbon dioxide ($CO_2$) as the main gaseous products. These gases were subsequently transformed into methane *via* catalytic methanation over a nickel-based catalyst under hydrogen atmosphere. The procedure ensured high reliability, with all experimental runs achieving mass balance closures above 95 wt%.

### 3.6. Catalytic evaluation tests

Catalytic cracking experiments were conducted in a microactivity test (MAT) unit designed to simulate the cyclic operation of industrial fluid catalytic cracking (FCC) reactors. The setup consisted of a fixed-bed reactor loaded with 3.0 g of catalyst, where the catalytic bed was positioned to ensure uniform flow and thermal distribution. Prior to each run, the catalyst samples were pretreated *in situ* under a continuous flow of dry air at 570 °C for 30 minutes to ensure complete removal of moisture and any adsorbed species, thus standardizing the initial conditions across all tests. The feedstock, a vacuum gas oil (VGO) with a controlled composition, was introduced at a constant mass flow rate of 2.0 g $min^{-1}$. To systematically study the catalytic performance under different catalyst-to-oil (C/O)

 

ratios, the contact time between the feed and the catalyst was varied by adjusting the residence time within the reactor, while maintaining constant feed and catalyst masses. Reaction temperatures were maintained at 550 °C, representative of commercial FCC riser conditions. Contact times of 20, 30, 40, and 50 seconds were selected to mimic a range of operational severities and to evaluate their impact on product distribution and catalyst activity. Reaction products were rapidly quenched and routed to a collection system for downstream analysis. Gaseous and liquid fractions were analyzed using a Shimadzu GC-2014 gas chromatograph equipped with a flame ionization detector (FID). The system employed a 30 m non-polar capillary column (250 μm internal diameter, 0.25 μm film thickness), enabling precise separation and quantification of hydrocarbon fractions ranging from light gases to gasoline range compounds. Conversion was calculated as the sum of the mass yields of dry gas (C1–C2), liquefied petroleum gas (LPG, C3–C4), gasoline (C5–216 °C) and coke fractions. In addition to conversion, the research octane number (RON) of the gasoline fraction was estimated using the correlation proposed by Anderson,[53] based on detailed hydrocarbon composition obtained from chromatographic data. Mass balance closures consistently exceeded 95% in all experimental runs, indicating high reliability of the measurements and negligible product loss. This ensured the reproducibility and robustness of the cracking results across different catalysts and operating conditions.

## 4. Conclusions

This study demonstrates that the strategic integration of hierarchical structuring and increased zeolite Y content in FCC catalysts offers a robust pathway to mitigate nitrogen-induced deactivation during the cracking of heavy Colombian VGO. The generation of intracrystalline mesoporosity not only enhances molecular diffusion and accessibility to acid sites but also contributes to the preservation of Brønsted acidity under chemically aggressive conditions. Catalysts containing 40 wt% hierarchical zeolites consistently outper-formed their conventional counterparts, exhibiting superior conversion, reduced coke formation, and improved gasoline selectivity even in the presence of strongly basic nitrogen compounds such as quinoline.

Importantly, the findings underscore the synergistic effect between pore architecture and active phase loading, suggesting that catalyst design must move beyond single-variable optimization toward more integrated approaches. While the use of model nitrogen compounds provided valuable mechanistic insights, future work should incorpo-rate real feedstock mixtures and regeneration cycles to validate long-term performance under industrial conditions.

Ultimately, this work contributes to the growing body of evidence supporting hierarchical zeolite engineering as a viable solution for refining operations facing increasingly complex and nitrogen-rich crude sources. The implications are particularly relevant for Latin American refineries, where the processing of unconventional feeds is both a challenge and an opportunity for innovation in catalyst technology.

## Author contributions

J. F. conceived the study and developed the methodology (conceptualization, methodology). M. L. O.-C.; D. M. and C. B.-A. conducted experiments and managed the data (investigation, data curation), performed statistical analyses and created visualizations (formal analysis, visualization). All authors contributed to writing the manuscript, with J. F. preparing the initial draft (writing – original draft) and J. D. G.; S. B.; R. V.-M. and F. E.-A. providing critical revisions (writing – review & editing). J. F. and F. E.-A. secured funding and supervised the project (funding acquisition, supervision, resources).

## Conflicts of interest

There are no conflicts of interest to declare.

## Data availability

Data for this article, including all data used for analysis and graphs, are available at https://data.mendeley.com at https://doi.org/10.17632/g3hx7hn8xm.1.

## Acknowledgements

The authors kindly acknowledge their respective Universities for providing kind support.

## References

1 D. Stratiev, I. Shishkova, M. Ivanov, I. Chavdarov and D. Yordanov, *Chem. Eng. Technol.*, 2020, **43**, 2266–2276.
2 G. Y. Nazarova, E. N. Ivashkina, B. J. Nafo, V. V. Maltsev and T. A. Shafran, *Bull. Tomsk Polytech. Univ.*, 2024, **335**, 172–184.
3 J. Fals, J. García, M. Falco and U. Sedran, *Fuel*, 2018, **225**, 26–34.
4 Z. Li, Q. Hu, Y. Qin, H. Liu, X. Zhao, X. Gao, L. Song and Z. Sun, *Ind. Eng. Chem. Res.*, 2022, **61**, 11628–11635.
5 S. Guo, S. Yu, H. Tian and Z. Da, *Fuel*, 2022, **324**, 124640.
6 J. Fals, J. García, M. Falco and U. Sedran, *Energy Fuels*, 2020, **34**, 16512–16521.
7 A. Ishihara, S. Matsuura, F. Hayashi, K. Suemitsu and T. Hashimoto, *Energy Fuels*, 2020, **34**, 7448–7454.
8 Y. Zhang, L. Wang, J. Yang, H. Chen and Y. Wang, *Catal. Sci. Technol.*, 2012, **2**, 1630–1638.
9 M. Niwa, K. Suzuki, N. Morishita, G. Sastre, K. Okumura and N. Katada, *Catal. Sci. Technol.*, 2013, **3**, 1919–1927.

10 T. V. Bobkova, V. P. Doronin, O. V. Potapenko, T. P. Sorokina and N. M. Ostrovskii, *Catal. Ind.*, 2014, **6**, 218–222.
11 G. Caeiro, P. Magnoux, J. M. Lopes, P. Ayrault and F. Ramôa Ribeiro, *J. Catal.*, 2007, **249**, 234–243.
12 H. S. Cerqueira, G. Caeiro, L. Costa and F. Ramôa Ribeiro, *J. Mol. Catal. A: Chem.*, 2008, **292**, 1–13.
13 N. Zambrano, D. Trueba, I. Hita, R. Palos, J. Azkoiti, A. Gutiérrez and P. Castaño, *ChemSusChem*, 2024, **17**, 15.
14 T. Lai, Y. Mao, W. Wang, X. Wang, N. Wang and Z. Liu, *Fuel*, 2020, **262**, 116523.
15 P. Bai, U. J. Etim, Z. Yan, S. Mintova, Z. Zhang, Z. Zhong and X. Gao, *Catal. Rev.*, 2019, **61**, 333–405.
16 L. Pérez, R. García, C. Martínez and A. López, *Fuel Process. Technol.*, 2020, **199**, 106251.
17 U. J. Etim, P. Bai, F. Subhan and Z. Yan, *Fuel*, 2016, **178**, 243–252.
18 J. Fals, M. L. Ospina-Castro, A. Ramos-Hernández, L. Pacheco-Londoño and S. Bocanegra, *Heliyon*, 2024, **10**, e37813.
19 A. Hernández-Giménez, E. Heracleous, E. Pachatouridou, A. Horvat, H. Hernando, D. Serrano, A. Lappas, P. Bruijnincx and B. Weckhuysen, *ChemCatChem*, 2021, **13**, 1207–1219.
20 H. Yu, J. Zang, G. Liu, M. Hong, R. Chen and T. Chen, *ACS Omega*, 2020, **5**, 18028–18034.
21 J. Fals, J. García-Valencia, E. Puello-Polo, F. Tuler and E. Márquez, *Molecules*, 2024, **29**, 3085.
22 F. Passamonti, G. De la Puente and U. Sedran, *Energy Fuels*, 2009, **23**, 1358–1363.
23 ASTM, ASTM D3907-03, 2008.
24 B. Behera, S. Ray and I. Singh, *Fuel*, 2008, **87**, 2322–2333.
25 L. Wei, H. Wang, Q. Dong, Y. Li and H. Xiang, *Catalysts*, 2025, **15**, 401.
26 G. Félix, A. Tirado, M. A. Varfolomeev, A. Al-muntaser, M. A. Suwaid, C. Yuan and J. Ancheyta, *Geoenergy Sci. Eng.*, 2023, 212242.
27 M. F. Abid, M. K. Abdullah and S. M. Ali, *Arabian J. Sci. Eng.*, 2017, **42**, x–y.
28 D. Wallenstein, D. Farmer, J. Knoell, C. Fougret and S. Brandt, *Appl. Catal., A*, 2013, **462–463**, 91–99.
29 J. García, J. Fals, L. Dietta and U. Sedran, *Fuel*, 2022, **328**, 125327.
30 G. Caeiro, P. Magnoux, J. M. Lopes and F. Ramôa Ribeiro, *Appl. Catal., A*, 2005, **292**, 189–199.
31 D. S. Oliveira, R. B. Lima, S. B. C. Pergher and V. P. S. Caldeira, *Catalysts*, 2023, **13**, 316.
32 J. Fals, E. Puello-Polo and E. Márquez, *Molecules*, 2024, **29**, 4753.
33 T. Barzetti, E. Selli, D. Moscotti and L. Forni, *J. Chem. Soc., Faraday Trans.*, 1996, **92**, 1401–1407.
34 D. Stratiev, I. Shishkova, M. Ivanov, R. Dinkov, B. Georgiev, G. Argirov, V. Atanassova, P. Vassilev, K. Atanassov, D. Yordanov, A. Popov, A. Padovani, U. Hartmann, S. Brandt, S. Nenov, S. Sotirov and E. Sotirova, *ACS Omega*, 2021, **6**, 7626–7637.
35 M. Moghaddam, A. Abbassi and J. Ghazanfarian, *Chem. Eng. Sci.*, 2022, **267**, 117240.
36 D. Han, N. Sun, J. Liu, C. Li, H. Shan and C. Yang, *Energy Chem.*, 2014, **23**, 519–526.
37 J. S. Bitters, T. He, E. Nestler, S. D. Senanayake, J. Chen and C. Zhang, *Energy Chem.*, 2024, **68**, 124–142.
38 ASTM, ASTM D2892-20, 2020.
39 M. Sarker, H. J. An and S. H. Jhung, *J. Phys. Chem. C*, 2018, **122**, 4532–4539.
40 C. M. Celis-Cornejo, D. J. Pérez-Martínez, J. A. Orrego-Ruiz and V. G. Baldovino-Medrano, *Energy Fuels*, 2018, **32**, 8715–8726.
41 J. Fals, L. Gutiérrez-Beleño and M. Jimenez-Rojas, *Innov. Cienc.*, 2022, **12**, 93–102.
42 ASTM, ASTM D287-12b, 2019.
43 ASTM, ASTM D4530-15, 2020.
44 ASTM, ASTM D2887-23, 2023.
45 ASTM, ASTM D2007-11, 2016.
46 ASTM, UOP714-07, 2007.
47 ASTM, ASTM D5291-21, 2021.
48 J. Fals, C. A. T. Toloza, E. Puello-Polo, E. Márquez and F. J. Méndez, *Heliyon*, 2023, **9**, e15408.
49 ASTM, ASTM D3906-03, 2013.
50 ASTM, ASTM D3942-19, 2019.
51 ASTM, ASTM D4222, 2015.
52 Á. Ibarra, A. Veloso, J. Bilbao, J. M. Arandes and P. Castaño, *Appl. Catal., B*, 2016, **182**, 336–346.
53 P. Anderson, J. Sharkey and R. Walsh, *J. Inst. Pet.*, 1972, **58**, 83–94.